Structures, energies, bonding, and NMR properties of pnicogen complexes H2XP:NXH2 (X ≥ H, CH3, NH2, OH, F, Cl)

ARTICLE *in* THE JOURNAL OF PHYSICAL CHEMISTRY A · NOVEMBER 2011

Impact Factor: 2.69 · DOI: 10.1021/jp2094164 · Source: PubMed

4 AUTHORS, INCLUDING:

Ibon Alkorta
Spanish National Research Council
679 PUBLICATIONS **12,389** CITATIONS
SEE PROFILE

Goar Sánchez
University College Dublin
69 PUBLICATIONS **900** CITATIONS
SEE PROFILE

José Elguero
Spanish National Research Council
1,502 PUBLICATIONS **22,151** CITATIONS
SEE PROFILE

THE JOURNAL OF PHYSICAL CHEMISTRY A

ARTICLE

pubs.acs.org/JPCA

Structures, Energies, Bonding, and NMR Properties of Pnicogen Complexes $H_2XP{:}NXH_2$ (X = H, CH_3, NH_2, OH, F, Cl)

Janet E. Del Bene,*[†] Ibon Alkorta,*[‡] Goar Sanchez-Sanz,[‡] and José Elguero[‡]

[†]Department of Chemistry, Youngstown State University, Youngstown, Ohio 44555, United States

[‡]Instituto de Química Médica, CSIC, Juan de la Cierva, 3, E-28006 Madrid, Spain

Supporting Information

ABSTRACT: Ab initio calculations have been carried out in a systematic investigation of P···N pnicogen complexes $H_2XP{:}NXH_2$ for X = H, CH_3, NH_2, OH, F, and Cl, as well as selected complexes with different substituents X bonded to P and N. Binding energies for complexes $H_2XP{:}NXH_2$ range from 8 to 27 kJ mol^{-1} and increase to 39 kJ mol^{-1} for $H_2FP{:}N(CH_3)H_2$. Equilibrium structures have a nearly linear A−P−N arrangement, with A being the atom directly bonded to P. Binding energies correlate with intermolecular N−P distances as well as with bonding parameters obtained from AIM and SAPT analyses. Complexation increases ^{31}P chemical shieldings in complexes with binding energies greater than 19 kJ mol^{-1}. One-bond spin−spin coupling constants $^{1P}J(N-P)$ across the pnicogen interaction exhibit a quadratic dependence on the N−P distance for complexes $H_2XP{:}NXH_2$, similar to the dependence of $^{2h}J(X-Y)$ on the X−Y distance for complexes with X−H···Y hydrogen bonds. However, when the mixed complexes $H_2XP{:}NX'H_2$ are included, the curvature of the trendline changes and the good correlation between $^{1P}J(N-P)$ and the N−P distance is lost.

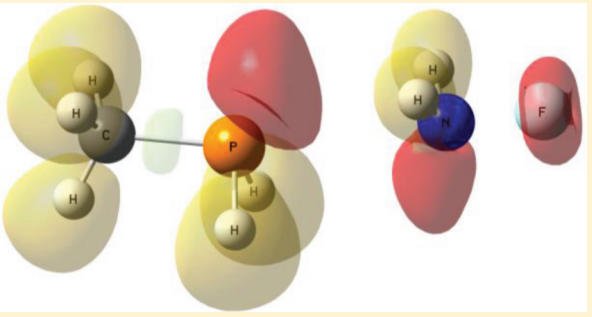

1. INTRODUCTION

The pnicogen bond has been recognized as a new and important type of intramolecular and intermolecular interaction.[1−3] In a recent paper, Hey-Hawkins et al. carried out a high-level theoretical study of the pnicogen P···P bond for a series of complexes and described the pnicogen bond as a new molecular linker.[4] Recently, we examined substituent effects in a series of complexes $(H_2XP)_2$, identified common structural characteristics, and demonstrated that one-bond P−P spin−spin coupling constants could be used to extract intermolecular P−P distances.[5]

Hey-Hawkins et al. also investigated an N···P pnicogen interaction in an aminoalkyl-ferrocenyldichlorophosphane.[6] Solimannejad et al. described the interaction of HSN with PH_3 and other phosphines.[7] These studies have been extended by Scheiner who carried out an examination of the bonding characteristics of complexes formed between substituted PH_3 molecules and NH_3.[8−10]

Given the new and unique character of the pnicogen bond and the scarcity of both experimental and theoretical NMR data for pnicogen complexes, we have extended our studies to a series of complexes derived from monosubstituted PH_3 and NH_3 molecules, represented as $H_2XP{:}NXH_2$, for X = H, CH_3, NH_2, OH, F, and Cl, and have also allowed different X bonded to N and P in selected complexes $H_2XP{:}NX'H_2$. Our aim is to determine the structures, binding energies, bonding characteristics, and NMR properties of these complexes, examine the extent to which they can be characterized by ^{15}N and ^{31}P chemical shieldings and $^{15}N-^{31}P$ spin−spin coupling constants, and compare these complexes to corresponding complexes $(H_2XP)_2$. In this Article, we present the results of this investigation.

2. METHODS

The structures of the monomers NH_2X and PH_2X for X = H, CH_3, NH_2, OH, F, and Cl, the complexes $H_2XP{:}NXH_2$, and selected mixed complexes $H_2FP{:}NClH_2$, $H_2FP{:}N(CH_3)H_2$, $H_2FP{:}NH_3$, $H_2ClP{:}NFH_2$, $H_2(CH_3)P{:}NFH_2$, and $H_3P{:}NFH_2$ were optimized at second-order Møller−Plesset perturbation theory (MP2)[11−14] with the aug′-cc-pVTZ basis set,[15] which is the Dunning aug-cc-pVTZ basis[16,17] without diffuse functions on H atoms. Frequency calculations were carried out to confirm that the optimized structures are local minima on their potential surfaces. The optimization and frequency calculations were carried out using Gaussian 09.[18] We have also evaluated the BSSE corrections for these complexes. While these reduce binding energies by 1 to as much as 4 kJ mol^{-1} for the most stable complexes, the order of stabilities remains the same, and the BSSE energies will not be discussed further in this Article.

Received: September 29, 2011
Revised: October 16, 2011
Published: November 02, 2011

Electron densities have been analyzed using the atoms in molecules (AIM) methodology[19,20] with the AIMPAC and AIMAll programs.[21,22] Electron density differences upon complex formation have been evaluated as the difference between the electron density of the complex and that of the isolated monomers at their geometry in the complex. The TOPMOD program[23] has been used to analyze the areas of charge concentration in terms of the Electron Localization Function (ELF).[24]

The Natural Bond Orbital (NBO) method[25] at the B3LYP/aug′-cc-pVTZ level has been employed to evaluate atomic charges using the NBO-3 program, and to analyze charge-transfer interactions involving occupied and unoccupied orbitals on N and P. Density Functional Theory-Symmetry Adapted Perturbation Theory (DFT-SAPT) calculations[26] have been carried out to evaluate the pnicogen interaction energy as a sum of electrostatic, exchange, induction, and dispersion terms. The SAPT interaction energy can be written as

$$E_{\text{int}} = E_{\text{el}}^{(1)} + E_{\text{ex}}^{(1)} + E_{\text{ind}}^{(2)} + E_{\text{ex-ind}}^{(2)} + E_{\text{disp}}^{(2)} + E_{\text{ex-disp}}^{(2)} + \delta(\text{HF}) \quad (1)$$

where $E_{\text{el}}^{(1)}$ is the electrostatic interaction energy of the two monomers each with its unperturbed electron distribution; $E_{\text{ex}}^{(1)}$ is the exchange energy, which is the first-order valence repulsion energy of the monomers due to the Pauli exclusion principle; $E_{\text{ind}}^{(2)}$ accounts for the second-order energy resulting from the induction interaction; $E_{\text{ex-ind}}^{(2)}$ is the change in the repulsion energy due to deformation of the electron cloud; $E_{\text{disp}}^{(2)}$ corresponds to the second-order dispersion energy; and $E_{\text{ex-disp}}^{(2)}$ is the second-order correction for coupling between the exchange-repulsion and the dispersion interactions. The δ(HF) term is a Hartree−Fock correction that includes higher order induction and exchange corrections not included in the other terms. All DFT-SAPT calculations have been carried out at PBE0/aug′-cc-pVTZ with the MOLPRO program.[27]

The NMR properties of the absolute chemical shieldings and spin−spin coupling constants have been evaluated for the pnicogen complexes. The absolute chemical shieldings have been calculated with the GIAO method[28] at MP2/aug′-cc-pVTZ using the Gaussian 09 program.[18] Indirect spin−spin coupling constants were computed using the equation-of-motion coupled cluster singles and doubles (EOM-CCSD) method in the CI(configuration interaction)-like approximation,[29,30] with all electrons correlated. For these calculations, the Ahlrichs[31] qzp basis set was placed on ^{13}C, ^{15}N, ^{17}O, and ^{19}F atoms and the qz2p basis set on ^{31}P and ^{35}Cl. The Dunning cc-pVDZ basis[16,17] was placed on H atoms. Analogous to the designation of coupling constants across hydrogen bonds, we designate the N−P coupling constants across pnicogen bonds as ^{1p}J(N−P). These coupling constants were evaluated as a sum of the paramagnetic spin−orbit (PSO), diamagnetic spin−orbit (DSO), Fermi-contact (FC), and spin-dipole (SD) terms.[32] The coupling constant calculations were carried out using ACES II[33] on the IBM 1350 cluster (Glenn) at the Ohio Supercomputer Center.

3. RESULTS AND DISCUSSION

3.1. Structures and Binding Energies. Total energies of monomers and pnicogen complexes are reported in Table S1 of the Supporting Information, and geometries are given in Table S2. Representative complexes are illustrated in Figure 1. Equilibrium structures have the H atoms of PXH_2 and NXH_2 trans with respect to the P−N axis and C_s symmetry, except for $H_2(NH_2)P{:}N(NH_2)H_2$, which has C_1 symmetry. Two stable C_1 structures with similar geometric and energetic properties were found for this complex, but only the more stable one has been included in this study.

Table 1 presents the intermolecular N−P distances, binding energies, and A−P−N and P−N−A angles, with A the atom of X (or X′) that is directly bonded to N or P. It was observed previously that pnicogen homodimers $(H_2XP)_2$ with P···P bonds have a nearly linear A−P···P−A alignment.[5] As is evident from Table 1, the A−P−N angle approaches linearity, with values between 160° and 172°. It would appear that this orientation can be traced to the structure of the PH_2X monomers in which the angle between the bisector of the H−P−H angle and the P−X bond is generally near 95°, and to the trans arrangement of PH_2 and NH_2 groups. In contrast, the P−N−A angle in these complexes is usually much smaller, although it is greater than the tetrahedral angle associated with an sp^3 hybridized N. However, there are four complexes in which the P−N−A angle is significantly increased, $H_3P{:}NH_3$ (155°), $H_2(CH_3)P{:}N(CH_3)H_2$ (163°), $H_3P{:}NFH_2$ (177°), and $H_2(CH_3)P{:}NFH_2$ (180°). These are the four most weakly bound pnicogen complexes with binding energies between 8 and 13 kJ mol^{-1}.

Why are these four complexes so weakly bound? From the binding energies in Table 1, it can be seen that the complex $H_2FP{:}NFH_2$ has the greatest binding energy. Indeed, it was observed previously that electron-rich groups bonded to P in pnicogen complexes with P···N bonds to NH_3 are very stable.[8] This might suggest that F-substitution increases the acidity of P. However, our recent study of complexes $(H_2XP)_2$ illustrates that these same electron-rich groups can be bonded to both P atoms, and that $(H_2FP)_2$ still has the greatest binding energy.[5] Moreover, F-substitution decreases the basicity of NH_3 in complexes with P···N pnicogen bonds. Thus, the stability of the pnicogen bond cannot be explained solely in terms of acidity and basicity based on the electron-donating and electron-withdrawing effects of substituents, although these effects certainly play a role. The structures of complexes $(H_2XP)_2$ have an essentially linear A−P···P−A alignment. Electron-rich substituents like F have nonbonded electron pairs, which can be polarized toward P. Mutual polarization results in an increased electron density in the region of the pnicogen bond and increased stability of these complexes.

To gain further insight into the pnicogen bond, we have investigated complexes in which different substituents are bonded to N and P, including $H_2ClP{:}NFH_2$, $H_2(CH_3)P{:}NFH_2$, $H_3P{:}NFH_2$, $H_2FP{:}N(CH_3)H_2$, $H_2FP{:}NClH_2$, and $H_2FP{:}NH_3$. The most strongly bound complexes are those with the strongest acid H_2FP bonded to the relatively strong bases $N(CH_3)H_2$ and NH_3. That the complex with $NClH_2$ as the base has the greatest binding energy among complexes in this group suggests that the electronegativeity of the substituent, in this case Cl with three nonbonded pairs of electrons, is an important factor in determining the stabilities of pnicogen

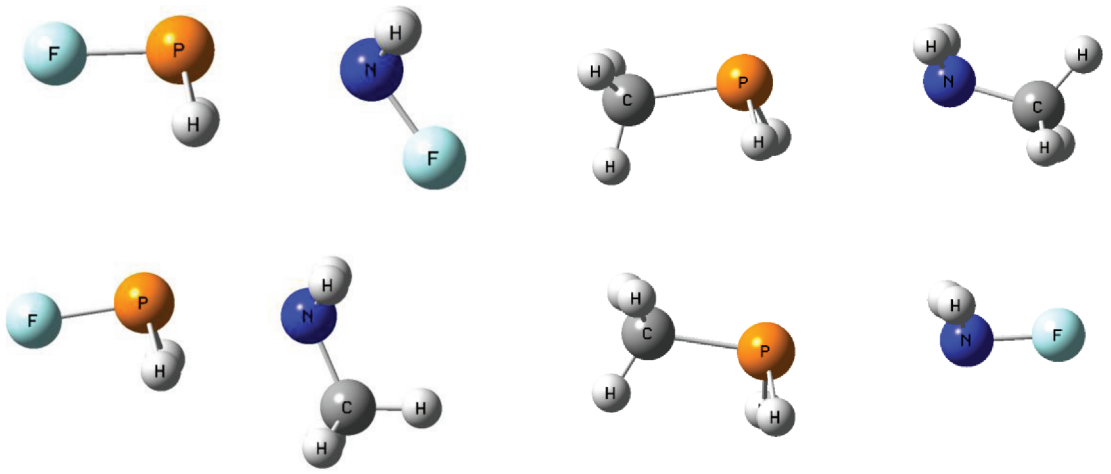

Figure 1. Representative pnicogen complexes.

Table 1. MP2/aug′-cc-pVTZ N−P Distances (R, Å), Angles A−P−N and P−N−A (deg), Binding Energies (ΔE, kJ mol^{-1}), and Spin−Spin Coupling Constants [^{1p}J(N−P), Hz] for Pnicogen Complexes with N−P Bonds

	R(N−P)	∠A−P−N[a]	∠P−N−A[a]	ΔE[b]	^{1p}J(N−P)
	Complexes $H_2XP{:}NXH_2$				
$H_2FP{:}NFH_2$	2.524	172	131	26.67	−113.6
$H_2ClP{:}NClH_2$	2.669	167	121	24.33	−90.8
$H_2(OH)P{:}N(OH)H_2$	2.750	160	112	19.23	−52.0
$H_2(NH_2)P{:}N(NH_2)H_2$	3.001	171	139	16.91	−39.7
$H_2(CH_3)P{:}N(CH_3)H_2$	3.257	172	163	8.64	−19.4
$H_3P{:}NH_3$	3.292	165	155	7.82	−17.5
	Complexes $H_2XP{:}NFH_2$				
$H_2ClP{:}NFH_2$	2.695	171	130	20.98	−105.0
$H_2(CH_3)P{:}NFH_2$	3.120	168	180	12.76	−67.9
$H_3P{:}NFH_2$	3.225	165	177	10.69	−33.1
	Complexes $H_2FP{:}NXH_2$				
$H_2FP{:}N(CH_3)H_2$	2.448	166	118	39.37	−41.3
$H_2FP{:}NH_3$	2.609	168	122	29.88	−65.6
$H_2FP{:}NClH_2$	2.543	169	126	29.08	−95.1

[a] A is the atom of X or X′ that is directly bonded to P or N. [b] ΔE is the negative energy for the reaction $H_2XP + NX'H_2 \rightarrow H_2XP{:}NX'H_2$.

complexes. The four complexes with the weakest pnicogen bonds are $H_3P{:}NH_3$, $H_2(CH_3)P{:}N(CH_3)H_2$, $H_3P{:}NFH_2$, and $H_2(CH_3)P{:}NFH_2$. All contain the relatively weak phosphourus acids PH_3 and $P(CH_3)H_2$. In two complexes, these acids are bonded to the relatively strong bases NH_3 and $N(CH_3)H_2$. However, in the other two complexes, it is the weakest base NFH_2 that forms the pnicogen bond. All four complexes have a common structural characteristic: both the A−P−N and the P−N−A angles approach linearity. In particular, when the weakest nitrogen base NFH_2 is present, the P−N−F angle increases to 177° and 180° in $H_3P{:}NFH_2$ and $H_2(CH_3)P{:}NFH_2$, respectively. This orientation of the base also allows for the approach of the H atoms of NXH_2 toward the region of increased electron density which constitutes the pnicogen bond. This can be seen in Figure 2 for $H_2(CH_3)P{:}NFH_2$.

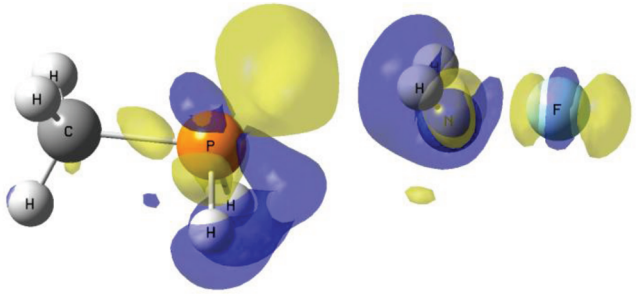

Figure 2. Electron density difference isosurface for $H_2(CH_3)P{:}NFH_2$ at ±0.003 au. Blue and yellow regions indicate regions of decreased and increased electron densities, respectively.

The intermolecular N−P distances in these complexes range from 2.448 to 3.292 Å and correlate well with binding energies, as illustrated in Figure 3. It is both interesting and unexpected that the N−P distance of 2.524 Å in $H_2FP{:}NFH_2$ is slightly greater than the P−P distance of 2.471 Å in the homodimer $(PFH_2)_2$ despite the larger van der Waals radius of P relative to N. The binding energy of 34 kJ/mol for $(PFH_2)_2$ is also greater than the binding energy of $H_2FP{:}NFH_2$ (26.7 kJ/mol). However, the N−P distances for the remaining $H_2XP{:}NXH_2$ complexes are shorter than the P−P distances in the corresponding $(H_2XP)_2$ complexes. The binding energies of the other corresponding complexes in the two series are similar. The N−P distances in the complexes are much longer than the N−P covalent bond distances of 1.720 and 1.766 Å, respectively, for the MP2/aug′-cc-pVTZ optimized equilibrium C_1 structure of $H_2N{-}PH_2$ and an optimized C_s trans structure.

3.2. ELF, AIM, and NBO Analyses. The ELF isosurfaces depicted in Figure 4 indicate that the lone pairs on nitrogen and phosphorus lie on opposite sides of the P···N bond. The local dipole moments associated with the lone pairs of P and N are antiparallel, which corresponds to a stabilizing arrangement. In addition, this alignment also allows for an attractive interaction between the lone pair of one molecule and the hydrogen atoms of the other. The NBO analysis also shows that in the most strongly bound complexes, the interaction of the N lone pair with the σ^* P−H orbital is small but detectable, similar to the situation found in hydrogen-bonded complexes.

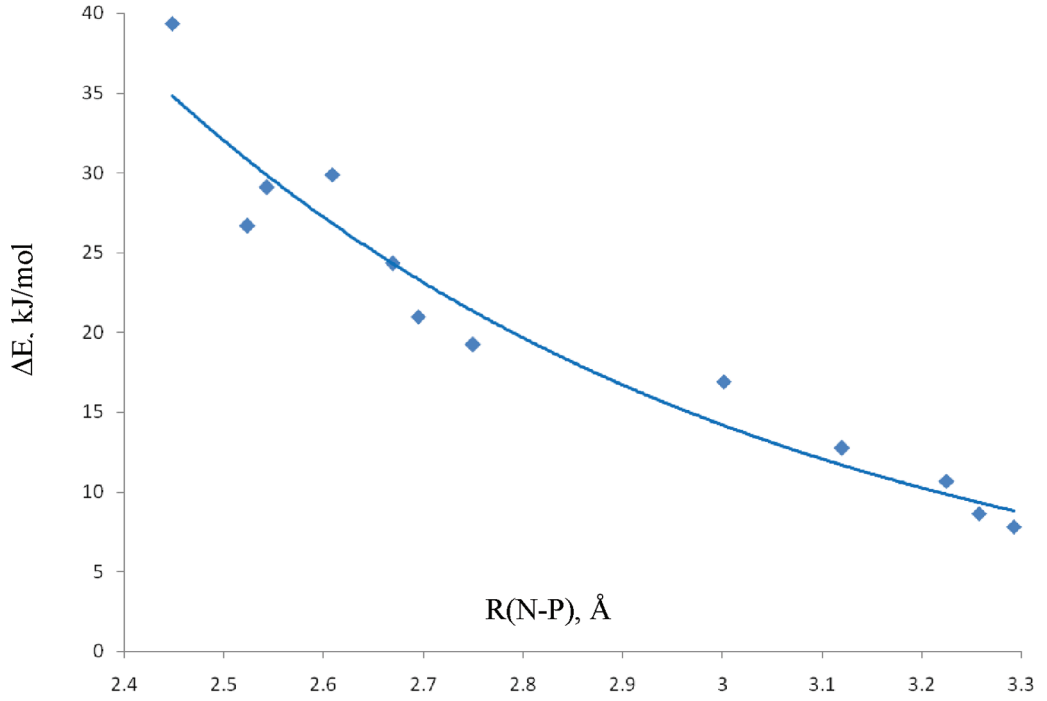

Figure 3. Binding energies of complexes $H_2XP{:}NXH_2$ and selected complexes $H_2XP{:}NX'H_2$ versus the N−P distance. The exponential relationship has a correlation coefficient of 0.954.

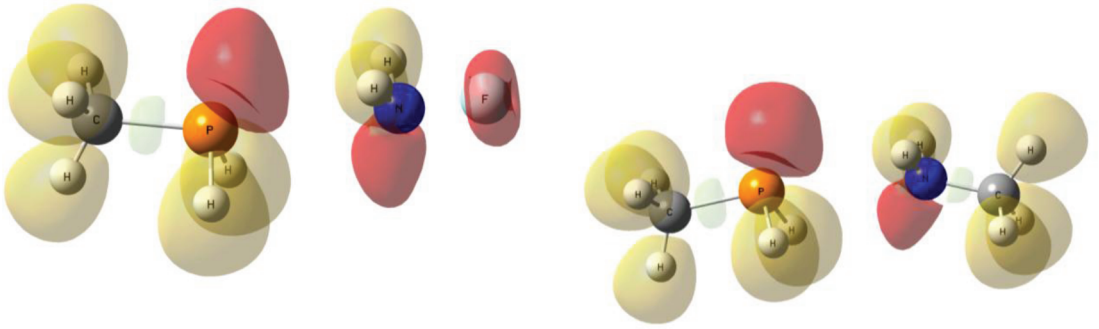

Figure 4. ELF isosurfaces for $H_2(CH_3)P{:}NFH_2$ and $H_2(CH_3)P{:}N(CH_3)H_2$ at 0.8 au. The lone pair regions are shown in red.

Table 2. AIM and NBO Charges and Second-Order Orbital Interaction Energies (kJ mol^{-1})

	charge (AIM) (PH_2X molecule)	charge (NBO) (PH_2X molecule)	$E(2)$ kJ mol^{-1} LP P→σ^*N−A[a]	$E(2)$ kJ mol^{-1} LP N→σ^*P−A[a]
$H_2FP{:}NFH_2$	−0.024	−0.048	12.1	53.9
$H_2ClP{:}NClH_2$	−0.030	−0.049	4.0	42.6
$H_2(OH)P{:}N(OH)H_2$	−0.023	−0.045	1.6	33.7
$H_2(NH_2)P{:}N(NH_2)H_2$	−0.014	−0.021	2.7	15.5
$H_2(CH_3)P{:}N(CH_3)H_2$	0.001	−0.009	1.5	4.9
$H_3P{:}NH_3$	−0.002	−0.008	1.7	6.5
$H_2ClP{:}NFH_2$	−0.021	−0.047	5.7	42.7
$H_2(CH_3)P{:}NFH_2$	0.022	0.006	6.4	4.7
$H_3P{:}NFH_2$	0.018	0.003	1.1	0.85
$H_2FP{:}N(CH_3)H_2$	−0.071	−0.099	*b*	
$H_2FP{:}NH_3$	−0.052	−0.070	0.9	11.55
$H_2FP{:}NClH_2$	−0.033	−0.046	8.8	47.4

[a] A is the heavy atom bonded to N or P except for NH_3 and PH_3. [b] This complex is unique insofar as the NBO method considers it to be a molecule.

dx.doi.org/10.1021/jp2094164 |*J. Phys. Chem. A* 2011, 115, 13724–13731

The NBO data of Table 2 show that upon complex formation, the phosphorus molecule gains electron density, except in the two weakly bound complexes $P(CH_3)H_2$:NFH_2 and H_3P:NFH_2 with NFH_2 as the base. The AIM charges are always more positive for the phosphorus molecule than those obtained with the NBO method, but both methods exhibit a similar pattern. The orbital interaction energies show that electron transfer can occur in both directions, from the lone pair on P to the σ^* N−X orbital, and from the lone pair on N to the σ^* P−X orbital. However, the amount of charge transfer from the lone pair on N to the σ^* P−X orbital is always greater, except for $H_2(CH_3)P$:NFH_2 and H_3P:NFH_2. This difference is consistent with the loss of electron density by the phosphorus molecules in these two complexes.

A surprising result of the NBO analysis is the description of the H_2FP:$N(CH_3)H_2$ complex as a single molecule. Although H_2FP:$N(CH_3)H_2$ has the strongest binding energy and the shortest P−N distance of 2.448 Å, this distance is clearly too long for a covalent bond, particularly when compared to the P−N distance of 1.720 Å in the H_2P-NH_2 molecule. Moreover, the calculated P−N bond order of H_2FP:$N(CH_3)H_2$ is only 0.19, as compared to a bond order of 0.91 for the H_2P-NH_2 molecule.

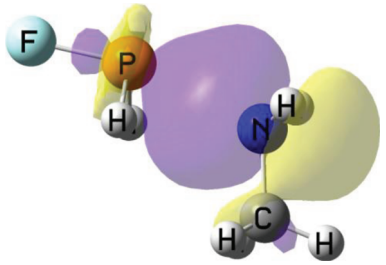

Figure 5. NBO HOMO of H_2FP:$N(CH_3)H_2$. The two colors differentiate positive and negative lobes.

We have also used the NBO method to examine the nature of the HOMO in these N···P complexes. In general, when X or X′ is F, Cl, OH, or NH_2, the HOMO is an orbital associated with the substituent. For both $H_2(CH_3)P$:$N(CH_3)H_2$ and H_3P:NH_3, the HOMO is a lone pair on N. For the H_2FP:$N(CH_3)H_2$ complex, the HOMO, which is illustrated in Figure 5, corresponds to a lone pair on N with a small (4%) contribution from P. This orbital is similar to those found in other donor−acceptor systems such as H_3B:NH_3 in which the bond forms between the lone pair of the electron-pair donor and an unoccupied orbital of the acceptor.

Analysis of the electron density shows the presence of a bond critical point (ρ_{BCP}) and a corresponding bond path, which links the phosphorus and nitrogen atoms in each complex. Values of the electron density at the BPC (0.040 to 0.008 au) and the Laplacian (0.068 to 0.025) indicate weak interactions within the closed shell regime. An exponential relationship is obtained between ρ_{BCP} and the interatomic N−P distance, as illustrated in Figure 6. Similar relationships have been found for a large variety of hydrogen-bonded complexes.[34] A linear relationship is also found between ρ_{BCP} and the binding energy, with a correlation coefficient of 0.95.

3.3. DFT-SAPT Analysis. The components of ΔE_{SAPT} reported in Table 3 show that the destabilizing exchange interaction $E_{ex}^{(1)}$ is the largest term contributing to the total energy. However, $E_{el}^{(1)}$, $E_{ind}^{(2)}$, $E_{ex\text{-}ind}^{(2)}$, $E_{disp}^{(2)}$, $E_{ex\text{-}disp}^{(2)}$, and δ(HF) are all stabilizing, and together account for the stability of the pnicogen complexes. The electrostatic term, $E_{el}^{(1)}$, is by far the most important of these, although for the least stable H_2XP:NXH_2 complexes, the dispersion energy $E_{disp}^{(2)}$ is comparable to the electrostatic energy. The induction component $E_{ind}^{(2)}$ and δ(HF) make similar contributions in all complexes except for the most strongly bound H_2FP:$N(CH_3)H_2$ complex, for which the induction energy is significantly greater. For complexes H_2XP:NXH_2 and H_2XP:NFH_2, the absolute values of

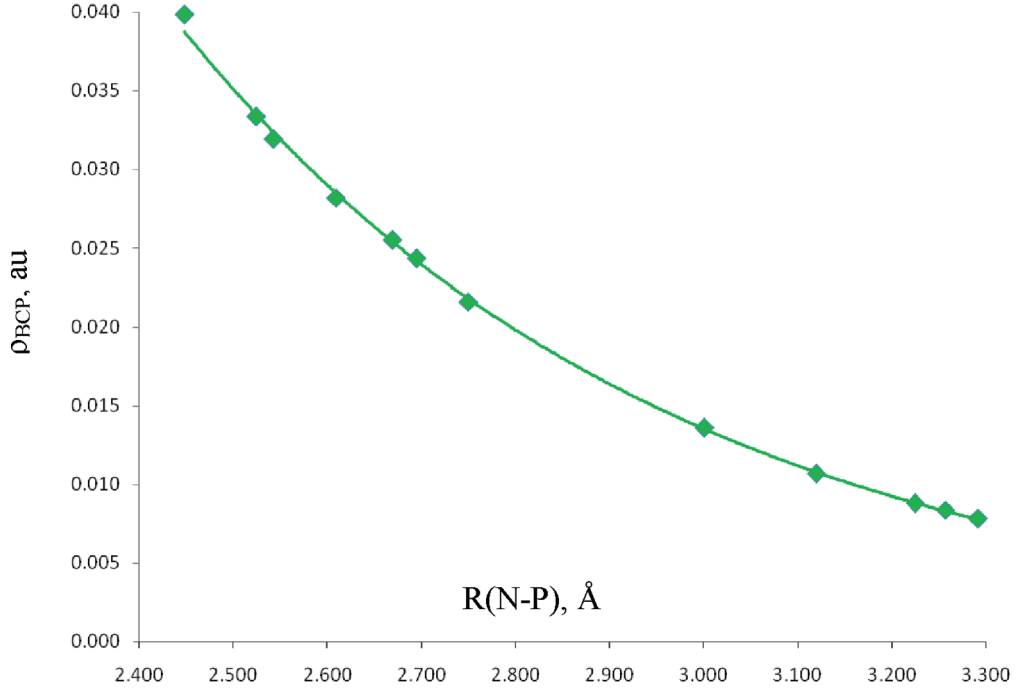

Figure 6. Electron density at the BCP versus the N−P distance. The exponential relationship has a correlation coefficient of 0.9996.

dx.doi.org/10.1021/jp2094164 |J. Phys. Chem. A 2011, 115, 13724–13731

Table 3. DFT-SAPT Components of the Interaction Energy for Pnicogen Complexes (kJ mol^{-1})

	$E_{el}^{(1)}$	$E_{ex}^{(1)}$	$E_{ind}^{(2)}$	$E_{disp}^{(2)}$	δ(HF)	ΔE_{SAPT}[a]
Complexes $H_2XP{:}NXH_2$						
$H_2FP{:}NFH_2$	−77.6	120.7	−16.3	−28.4	−15.1	−16.7
$H_2ClP{:}NClH_2$	−54.2	84.6	−10.5	−25.8	−10.7	−16.6
$H_2(OH)P{:}N(OH)H_2$	−47.9	76.6	−8.6	−24.5	−8.0	−12.3
$H_2(NH_2)P{:}N(NH_2)H_2$	−24.8	38.4	−3.3	−15.7	−3.7	−9.1
$H_2(CH_3)P{:}N(CH_3)H_2$	−12.0	18.8	−1.3	−10.9	−1.5	−6.9
$H_3P{:}NH_3$	−11.2	16.2	−1.5	−8.7	−1.2	−6.4
Complexes $H_2XP{:}NFH_2$						
$H_2ClP{:}NFH_2$	−51.1	77.2	−9.0	−21.9	−9.7	−14.5
$H_2(CH_3)P{:}NFH_2$	−19.0	25.0	−1.4	−11.8	−3.4	−10.7
$H_3P{:}NFH_2$	−14.0	18.0	−1.2	−9.5	−2.4	−9.1
Complexes $H_2FP{:}NXH_2$						
$H_2FP{:}N(CH_3)H_2$	−117.8	180.1	−32.9	−39.6	−19.7	−29.9
$H_2FP{:}NH_3$	−75.0	107.7	−16.4	−26.2	−13.3	−23.2
$H_2FP{:}NClH_2$	−73.3	115.3	−15.9	−30.3	−14.5	−18.6

[a] ΔE_{SAPT} is the SAPT energy for the reaction $H_2XP + NX'H_2 \rightarrow H_2XP{:}NX'H_2$.

Table 4. Computed ^{31}P and ^{15}N Chemical Shieldings for Monomers and Complexes

	complex		isolated monomer	
	σ_P	σ_N	σ_P	σ_N
Complexes $H_2XP{:}NXH_2$				
$H_2FP{:}NFH_2$	339.70	79.92	272.76	77.56
$H_2ClP{:}NClH_2$	440.67	238.52	420.43	244.28
$H_2(OH)P{:}N(OH)H_2$	363.39	154.43	340.25	155.22
$H_2(NH_2)P{:}N(NH_2)H_2$	450.73	216.76	452.43	222.00
$H_2(CH_3)P{:}N(CH_3)H_2$	539.59	255.72	548.57	262.43
$H_3P{:}NH_3$	623.91	271.63	633.25	276.90
Complexes $H_2XP{:}NFH_2$				
$H_2ClP{:}NFH_2$	439.11	80.94	420.43	77.56
$H_2(CH_3)P{:}NFH_2$	543.02	76.05	548.57	77.56
$H_3P{:}NFH_2$	626.86	75.95	633.25	77.56
Complexes $H_2FP{:}NXH_2$				
$H_2FP{:}N(CH_3)H_2$	371.07	244.41	272.76	262.43
$H_2FP{:}NH_3$	349.46	266.91	272.76	276.90
$H_2FP{:}NClH_2$	337.71	236.22	272.76	244.28

each component decrease as the binding energies decrease, except for an interchange involving the weakly bound complexes $H_2(CH_3)P{:}N(CH_3)H_2$ and $H_3P{:}NH_3$. For complexes $H_2FP{:}NH_3$ and $H_2FP{:}NClH_2$, $E_{ex}^{(1)}$, $E_{disp}^{(2)}$, and δ(HF) are interchanged relative to ΔE_{SAPT}.

3.4. Chemical Shieldings. The calculated absolute chemical shieldings of the phosphorus and nitrogen atoms in monomers and complexes are reported in Table 4. The ^{31}P absolute chemical shieldings range between 633 and 273 ppm in the isolated monomers, and between 627 and 338 ppm in the complexes. Relative to the monomers, complexation increases the ^{31}P absolute chemical shieldings in those complexes with binding energies greater than 19 kJ mol^{-1}, which are also the complexes with significantly increased negative charges on the PH_2X molecules. The largest effects are observed in complexes formed with PFH_2. In particular, the ^{31}P chemical shielding increases by 98 ppm in the most strongly bound complex, $H_2FP{:}N(CH_3)H_2$. However, no correlations are found between ^{31}P chemical shifts and the bonding properties of these complexes.

The ^{15}N shieldings range between 277 and 78 ppm in the isolated molecules and between 272 and 76 ppm in the complexes. The effect of complexation leads to changes ranging from 4 to −18 ppm in the ^{15}N shieldings. However, even though the largest changes are found in the most strongly bound complexes, no relationships are found between changes in chemical shieldings upon complexation and complex binding energies.

3.5. Coupling Constants. Table 1 also reports coupling constants ^{1P}J(N−P) for the pnicogen complexes, and the components of ^{1P}J(N−P) are reported in Table S3 of the Supporting Information. These data show that the FC term is an excellent approximation to ^{1P}J(N−P). Thus, the N−P coupling constant depends on ground-state s electron densities and on s electron densities in excited triplet states, which couple to the ground state through the FC operator.

^{1P}J(N−P) varies from 18 Hz for $H_3P{:}NH_3$ to 114 Hz for $H_2FP{:}HFH_2$. Figure 7 presents a plot of ^{1P}J(N−P) versus the N−P distance for complexes with the same substituent bonded to both N and P. For these, ^{1P}J(N−P) increases quadratically as the intermolecular N−P distance decreases, with a correlation coefficient of 0.955. The distance dependence of ^{1P}J(N−P) across these N···P pnicogen bonds resembles the X−Y distance dependence of ^{2h}J(X−Y) across X−H···Y hydrogen bonds. For these pnicogen complexes, experimental N−P distances could be extracted from values of ^{1P}J(N−P). However, when the mixed complexes $H_2XP{:}NX'H_2$ are added, the curvature of the trendline changes, and the correlation between ^{1P}J(N−P) and the N−P distance is lost, as is also illustrated in Figure 7. It is interesting to note that when all complexes are included, the points for the four complexes that lie above the trendline at short N−P distances correspond to the four complexes with F and/or Cl bonded to P and N. These halogen substituents have three nonbonded pairs of electrons, which may enhance the s electron densities of both N and P in the ground state and in excited states that couple to the ground state, thereby leading to increased values of ^{1P}J(N−P).

^{1P}J(N−P) values for pnicogen complexes are negative. Because the magnetogyric ratio of ^{15}N is negative and that of ^{31}P is positive, the reduced coupling constants ^{1P}K(N−P) are positive, as are ^{1P}K(P−P) for the pnicogen homodimers $(H_2XP)_2$. A positive value of a one-bond coupling constant follows the Dirac Vector Model, which states that reduced one-bond couplings are positive.[35]

^{1P}J(N−P) for the pnicogen complexes can be compared to ^{1}J(N−P) for the $H_2P{-}NH_2$ molecule. A previous study of one-bond coupling constants in molecules $H_mX{-}YH_n$ including $H_2P{-}NH_2$ found that ^{1}J(X−Y) is extremely sensitive to rotation around the X−Y bond.[36] This can also be seen from the values of ^{1}J(N−P) and their components in Table 5 for the equilibrium C_1 structure of $H_2P{-}NH_2$ and for an optimized C_s trans structure. The largest component of ^{1}J(N−P) for the trans structure is a

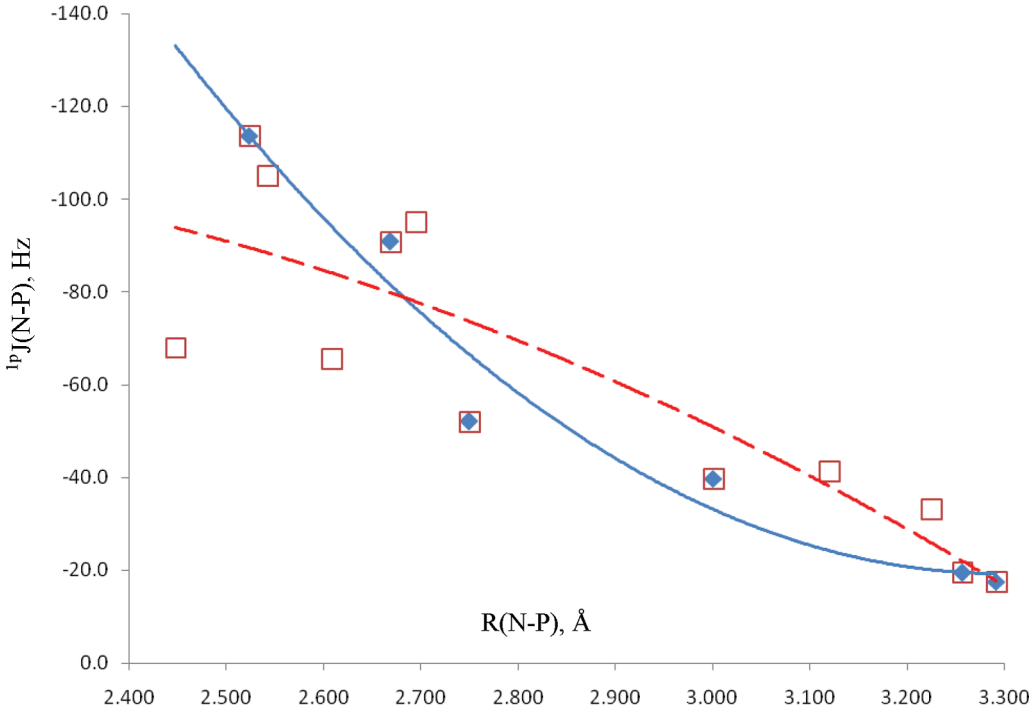

Figure 7. $^{1p}J(N-P)$ versus $R(N-P)$ for the pnicogen complexes $H_2XP:NXH_2$ (blue ◆ and solid line) and the entire set of complexes including $H_2XP:NX'H_2$ (red □ and dashed line).

Table 5. N−P Distance (R, Å) and $^1J(N-P)$ and Its Components (Hz) for H_2N-PH_2

sym	R	PSO	DSO	FC	SD	$^1J(N-P)$
C_s[a]	1.766	−2.7	0.0	12.9	−5.1	5.1
C_i[b]	1.721	2.0	0.0	46.3	−2.7	45.6

[a] MP2/aug′-cc-pVTZ optimized C_s trans structure [b] MP2/aug′-cc-pVTZ optimized C_1 equilibrium structure

positive FC term, followed by smaller negative PSO and SD terms. The partial cancellation of these terms results in a small value of 5.1 Hz for $^1J(N-P)$ in the C_s structure of this molecule. In contrast, the FC term is dominant and positive for the equilibrium C_1 structure and is an excellent approximation to the value of $^1J(N-P)$ of 45.6 Hz.

4. CONCLUSIONS

Ab initio calculations have been carried out in a systematic investigation of pnicogen complexes $H_2XP:NXH_2$ for X = H, CH_3, NH_2, OH, F, and Cl, and selected complexes $H_2XP:NX'H_2$ with different substituents bonded to N and P. Among complexes $H_2XP:NXH_2$, the N−P distances range from 2.524 Å in $H_2FP:NFH_2$ to 3.292 Å in $H_3P:NH_3$. The N−P distance in $H_2FP:NFH_2$ is greater than the P−P distance of 2.471 Å in $(PFH_2)_2$ despite the larger van der Waals radius of P. The N−P distances in the complexes are much longer than the N−P covalent bond distance in H_2N-PH_2. Equilibrium structures have a nearly linear A−P−N arrangement, with A the atom of X directly bonded to P. Complexes with small binding energies also have a linear or nearly linear P−N−A arrangement.

Binding energies correlate with intermolecular N−P distances, and with bonding parameters obtained from NBO, SAPT, and AIM analyses. These parameters indicate that both H_2XP and NXH_2 are electron-pair donors and acceptors via $P_{lp}\rightarrow\sigma^*_{N-X}$ and $N_{lp}\rightarrow\sigma^*_{P-X}$ charge-transfer interactions, with the former being dominant except in two weakly bound complexes. The electrostatic interaction is the dominant attractive interaction that stabilizes these complexes. As anticipated, there is an increase in electron density in the N···P bonding region.

Large variations in the ^{31}P chemical shieldings are observed upon complexation. Complexation increases ^{31}P chemical shieldings in complexes with binding energies greater than 19 kJ mol^{-1}.

One-bond spin−spin coupling constants $^{1p}J(N-P)$ across the pnicogen bond exhibit a quadratic dependence on the N−P distance for complexes $H_2XP:NXH_2$, similar to the dependence of $^{2h}J(X-Y)$ on the X−Y distance for complexes with X−H···Y hydrogen bonds. However, when the mixed complexes $H_2XP:NX'H_2$ are included, the curvature of the trendline changes and the correlation between $^{1p}J(N-P)$ and the N−P distance is lost. The FC term is an excellent approximation to $^{1p}J(N-P)$, which indicates that N−P coupling depends on s electron densities in both the ground state and the excited triplet states that couple to it.

■ ASSOCIATED CONTENT

Supporting Information. Complete refs 18, 27, 32. Geometries, energies, and PSO, DSO, FC, and SD components of $^1J(N-P)$. This material is available free of charge via the Internet at http://pubs.acs.org.

■ AUTHOR INFORMATION

Corresponding Author

*E-mail: jedelbene@ysu.edu (J.E.D.B.); ibon@iqm.csic.es (I.A.).

■ ACKNOWLEDGMENT

We thank the Ministerio de Ciencia e Innovación (Project No. CTQ2009-13129-C02-02) and the Comunidad Autónoma de Madrid (Project MADRISOLAR2, ref S2009/PPQ-1533) for continuing support. Thanks are due to the Ohio Supercomputer Center for continuing support of this research, and to the CTI (CSIC) for an allocation of computer time.

■ REFERENCES

(1) Sundberg, M. R.; Uggla, R.; Viñas, C.; Teixidor, F.; Paavola, S.; Kivekäs, R. *Inorg. Chem. Commun.* **2007**, *10*, 713.
(2) Tschirschwitz, S.; Lönnecke, P.; Hey-Hawkins, E. *Dalton Trans.* **2007**, 1377.
(3) Bauer, S.; Tschirschwitz, S.; Lönnecke, P.; Franck, R.; Kirchner, B.; Clarke, M. L.; Hey-Hawkins, E. *Eur. J. Inorg. Chem.* **2009**, 2776.
(4) Zahn, S.; Franck, R.; Hey-Hawkins, E.; Kirchner, B. *Chem.-Eur. J.* **2011**, *17*, 6034.
(5) Del Bene, J. E.; Alkorta, I.; Sánchez-Sanz, G.; Elguero, J. *Chem. Phys. Lett.* **2011**, *512*, 184.
(6) Tschirschwitz, S.; Lönnecke, P.; Hey-Hawkins, E. *Dalton Trans.* **2007**, 1377.
(7) Solimannejad, M.; Gharabaghi, M.; Scheiner, S. *J. Chem. Phys.* **2011**, *134*, 024312.
(8) Scheiner, S. *J. Chem. Phys.* **2011**, *134*, 094315.
(9) Scheiner, S. *Chem. Phys.* **2011**, *387*, 79.
(10) Scheiner, S. *J. Phys. Chem. A.* **2011**, *115*, 11202.
(11) Pople, J. A.; Binkley, J. S.; Seeger, R. *Int. J. Quantum Chem., Quantum Chem. Symp.* **1976**, *10*, 1.
(12) Krishnan, R.; Pople, J. A. *Int. J. Quantum Chem.* **1978**, *14*, 91.
(13) Bartlett, R. J.; Silver, D. M. *J. Chem. Phys.* **1975**, *62*, 3258.
(14) Bartlett, R. J.; Purvis, G. D. *Int. J. Quantum Chem.* **1978**, *14*, 561.
(15) Del Bene, J. E. *J. Phys. Chem.* **1993**, *97*, 107.
(16) Dunning, T. H., Jr. *J. Chem. Phys.* **1989**, *90*, 1007.
(17) Woon, D. E.; Dunning, T. H., Jr. *J. Chem. Phys.* **1995**, *103*, 4572.
(18) Frisch, M. J.; et al. *Gaussian 09*; Gaussian, Inc.: Wallingford, CT, 2009.
(19) Bader, R. F. W. In *Atoms in Molecules: A Quantum Theory*; The International Series of Monographs of Chemistry; Halpen, J., Green, M. L. H., Eds.; Clarendon Press: Oxford, 1990.
(20) Popelier, P. L. A. *Atoms in Molecules: An Introduction*; Prentice Hall: New York, 2000.
(21) AIMPAC: Bieger-Konig, F. W.; Bader, R. F. W.; Tang, T. H. *J. Comput. Chem.* **1982**, *3*, 317.
(22) Keith, T. A. AIMAll program, Version 11.04.03.
(23) Noury, S.; Krokidis, X.; Fuster, F.; Silvi, B. *ToPMoD*; Universite Pierre et Marie Curie: Paris, 1999.
(24) Silvi, B.; Savin, A. *Nature* **1994**, *371*, 683.
(25) Reed, A. E.; Curtiss, L. A.; Weinhold, F. *Chem. Rev.* **1988**, *88* 899.
(26) Chałasiński, G.; Szcześniak, M. M. *Chem. Rev.* **2000**, *100*, 4227.
(27) Werner, H. J.; et al. *Molpro-2010*; Cardiff, UK, 2010.
(28) Ditchfield, R. *Mol. Phys.* **1974**, *27*, 789.
(29) Perera, S. A.; Sekino, H.; Bartlett, R. J. *J. Chem. Phys.* **1994**, *101* 2186.
(30) Perera, S. A.; Nooijen, M.; Bartlett, R. J. *J. Chem. Phys.* **1996**, *104* 3290.
(31) Schäfer, A.; Horn, H.; Ahlrichs, R. *J. Chem. Phys.* **1992**, *97*, 2571.
(32) Kirpekar, S.; Jensen, H. J. Aa.; Oddershede, J. *Chem. Phys.* **1994**, *188*, 171.
(33) ACES II is a program product of the Quantum Theory Project, University of Florida. Authors: Stanton, J. F.; et al. Integral packages included are VMOL (Almlof, J.; Taylor, P. R.), VPROPS (Taylor, P. R.), and ABACUS (Helgaker, T.; Jensen, H. J. Aa.; Jorgensen, P.; Olsen, J.; Taylor, P. R.). Brillouin−Wigner perturbation theory was implement by: Pittner, J.
(34) Mata, I.; Alkorta, I.; Molins, E.; Espinosa, E. *Chem.-Eur. J.* **2010**, *16*, 2442.
(35) Lynden-Bell, R. M.; Harris, R. K. *Nuclear Magnetic Resonance Spectroscopy*; Appleton Century Crofts: New York, 1969.
(36) Del Bene, J. E.; Elguero, J. *J. Phys. Chem. A* **2006**, *110*, 12543.